Dalton Transactions



PAPER View Article Online



Cite this: *Dalton Trans.*, 2021, **50**, 12970

Received 3rd July 2021, Accepted 7th August 2021 DOI: 10.1039/d1dt02213j

rsc li/dalton

NMR studies of group 8 metallodrugs: ¹⁸⁷Os-enriched organo-osmium half-sandwich anticancer complex[†]

Russell J. Needham, (D) Ivan Prokes, (D) Abraha Habtemariam, (D) Isolda Romero-Canelón, (D) : Guy J. Clarkson (D) and Peter J. Sadler (D) *

We report the synthesis of the organo-osmium anticancer complex $[Os(\eta^6-p-cym)(N,N-azpy-NMe_2)Br]$ PF₆ (1) containing natural abundance ¹⁸⁷Os (1.96%), and isotopically-enriched (98%) [¹⁸⁷Os]-1. Complex 1 and [¹⁸⁷Os]-1 contain a π -bonded *para*-cymene (p-cym), a chelated 4-(2-pyridylazo)-N,N-dimethylaniline (azpy-NMe₂), and a monodentate bromide as ligands. The X-ray crystal structure of 1 confirmed its half-sandwich 'piano-stool' configuration. Complex 1 is a member of a family of potent anticancer complexes, and exhibits sub-micromolar activity against A2780 human ovarian cancer cells (IC₅₀ = 0.40 μ M). Complex [¹⁸⁷Os]-1 was analysed by high-resolution ESI-MS, 1D ¹H and ¹³C NMR, and 2D ¹H COSY, ¹³C-¹H HMQC, and ¹H-¹⁸⁷Os HMBC NMR spectroscopy. Couplings of ¹H and ¹³C nuclei from the azpy/p-cym ligands to ¹⁸⁷Os were observed with J-couplings (1J to 4J) ranging between 0.6–8.0 Hz. The ¹⁸⁷Os chemical shift of [¹⁸⁷Os]-1 (–4671.3 ppm, determined by 2D ¹H-¹⁸⁷Os HMBC NMR) is discussed in relation to the range of values reported for related Os(II) arene and cyclopentadienyl complexes (–2000 to –5200 ppm).

Introduction

There is much current interest in the design of transition metal anticancer complexes.¹⁻⁴ Progress depends on the elucidation of structure-activity relationships and their mechanisms of action, depends on the identification of their pharmacophores, the active species. Although some metal complexes are relatively inert (e.g. low-spin d⁶ complexes), many are pro-drugs which will undergo ligand exchange and redox reactions before reaching the target site. NMR is a potentially powerful method for investigating metallodrug speciation, since studies can be carried out in solution under physiologically relevant conditions, and information on the thermodynamics (equilibria) and kinetics (dynamics) of ligand exchange reactions can often be obtained. Direct observation of NMR resonances for the metals themselves (heteronuclear

NMR) is potentially very informative, but often difficult to achieve.

We focus here on group 8 transition metals, Fe, Ru and Os. In particular two Ru(III) complexes, NAMI-A ([trans-RuCl₄(DMSO-S)(Im)]ImH, where Im = imidazole) and KP1019 $([trans-RuCl_4(In)_2]InH, where In = indazole)$ have been on clinical trials. 5 Ru(III) complexes are paramagnetic, but diamagnetic low-spin 4d⁶ Ru(II) complexes, can in principle, be studied by 99Ru and 101Ru NMR, Table 1. Their natural abundances are reasonable (12.76% and 17.06%, respectively), and although their gyromagnetic ratios are relatively low, they should be detectable with similar sensitivities as 13C. However, both are quadrupolar with $I = \frac{5}{2}$; ¹⁰¹Ru has a higher quadrupole moment than 99Ru. Both isotopes give rise to broad lines unless in highly symmetrical complexes. The complexes [Ru $(NH_3)_6$ Cl₂ and K_4 Ru(CN)₆ (notably with a temperature coefficient for the chemical shift of >1 ppm K⁻¹) give narrow resonances and are useful references. 6 99Ru solution studies on such symmetrical complexes are also possible. For tris-(polypyridyl)Ru(II) complexes in acetonitrile, a correlation between the 99Ru-NMR chemical shifts and the energy of metal-toligand charge transfer has been reported.8 The chemical shift range for ⁹⁹Ru is >9000 ppm. The ⁹⁹Ru NMR linewidth of 0.15 M [Ru^{II}(bipyridine)₃]PF₆ in CD₃CN is 65 Hz, and for other polypyridyl complexes up to 800 Hz, depending on the

Department of Chemistry, University of Warwick, Gibbet Hill Road, Coventry CV4 7AL, UK. E-mail: P.J.Sadler@warwick.ac.uk

 $[\]dagger$ Electronic supplementary information (ESI) available. CCDC 2067332. For ESI and crystallographic data in CIF or other electronic format see DOI: 10.1039/d1dt02213j

[‡]Current address: School of Pharmacy, Institute of Clinical Sciences, University of Birmingham, Birmingham B15 2TT, UK.

Dalton Transactions Paper

Table 1 Properties of isotopes of group 8 transition metals which possess a nuclear spin¹²

Metal	Isotope	Abundance (%)	Nuclear spin (I)	Quadrupole moment ^a	$Frequency^b$	Receptivity ^c (Rel. to ¹³ C)
Iron	⁵⁷ Fe	2.119	1/2	_	12.955	4.25×10^{-3}
Ruthenium	⁹⁹ Ru ¹⁰¹ Ru	12.76 17.06	5/2 5/2	7.9 45.7	16.427 12.750	0.85 1.58
Osmium	¹⁸⁷ Os ¹⁸⁹ Os	1.96 16.15	1/2 3/2	— 85.6	9.132 31.072	$1.43 \times 10^{-3} $ 2.32

^a Electric quadrupole moment in units of fm² (10⁻³⁰ m²; 1 barn = 100 fm²). ^{b 1}H 400 MHz, ¹³C 100 MHz, ^c Receptivity at natural abundance relative to ¹³C.

counter-anion and concentration.9 There is medical interest in related complexes as photodynamic agents for the treatment of cancer. TLD-1433, [Ru(4,4'-dimethyl-2,2'-bipyridine)₂(2-(2',2'':5'',2'''-terthiophene)-imidazo[4,5-f][1,10]phenanthroline)] Cl₂, an octahedral tris-diimine Ru(II) complex with two methylated bipyridyl and one phenanthroline derivative as ligands, is activated by green light and currently on clinical trial for treatment of non-muscle invasive bladder cancer (NMIBC), which is refractory to Bacillus Calmette-Guérin (BCG) treatment. 10,11 Complexes of lower symmetry, such as half-sandwich Ru(II) arene anticancer complexes give resonances which are usually too broad to observe easily (unpublished data).

Although both Ru(II) and Ru(III) complexes have been widely explored as anticancer agents, similar studies of osmium complexes are more recent. 13-15 Os(vI) complexes, of general formula $[Os\{N\}(N^N)Cl_3]$ (where $N^N = 2,2'$ -bipyridine or a phenanthroline derivative), can attack DNA and induce endoplasmic reticulum stress, probably through

binding.16,17 Half sandwich diamine Os(II) arene anticancer complexes can also bind to DNA and inhibit DNA synthesis, 18-20 whereas azopyridine complexes are more inert and have a redox mechanism of action. Particularly potent is the iodido complex $[Os(\eta^6-p-cym)(N,N-azpy-NMe_2)I]PF_6$ (FY26; p-cym = para-cymene, azpy-NMe₂ = 2-(p-((dimethylamino)phenylazo)pyridine), which is ca. $49\times$ more active on average than the anticancer drug cisplatin towards a Sanger Institute panel of over 800 cancer cell lines, and induces formation of reactive oxygen species (ROS) in cancer cells. 21,22 This complex is capable of delaying the growth of HCT-116 human colon cancer xenografts in mice,23 and is up to 64× more selective towards A2780 ovarian cancer cells over normal cells when applied synergistically with L-buthionine sulfoximine, which blocks glutathione (γ-L-Glu-L-Cys-Gly, GSH) synthesis.²⁴ The complex FY26 is inert to hydrolysis, but undergoes activation in cancer cells by attack on the azo bond by the intracellular thiol GSH, resulting in liberation of the iodido ligand.²⁵

Scheme 1 The multi-step synthesis of $[^{187}Os(\eta^6-p-cym)(N,N-azpy-NMe_2)Br]PF_6$ with ^{187}Os isotopic enrichment, starting from ^{187}Os metal powder.

Additional current interest in organo-osmium(II) half sandwich complexes arises from their activity as transfer hydrogenation catalysts. For example, chiral arene (p-toluenesulfonyl)-1,2-diphenylethylenediamine (TsDPEN) complexes, [Os(arene) (TsDPEN)], are effective catalysts for the conversion of the natural metabolite pyruvate into either natural L-lactate or unnatural D-lactate depending on the enantiomer of the catalyst

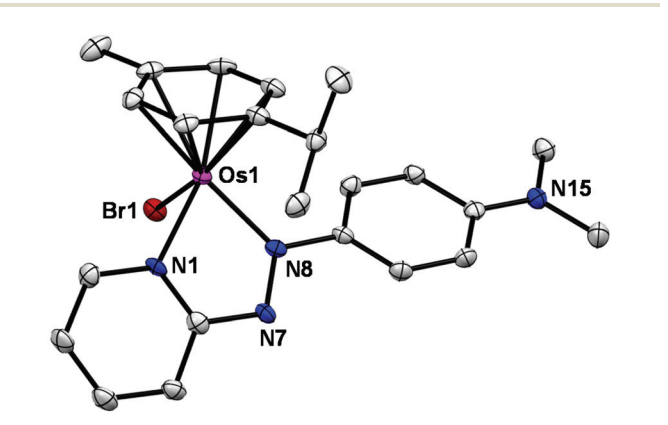


Fig. 1 ORTEP diagram for the cation in the X-ray crystal structure of $[Os(\eta^6-p-cym)(azpy-NMe_2)Br]PF_6$. Ellipsoids are shown at the 50% probability level and all hydrogens, counter ions and solvent molecules have been omitted for clarity.

used, reactions of which can be achieved even inside cancer cells. 26,27

Osmium NMR studies are highly challenging, firstly, the natural abundance in the Earth's crust is very low, ca. 1 g per 200 tonnes, making it amongst the rarest stable elements in the periodic table.²⁸ There are seven stable naturally-occurring osmium isotopes:²⁹ ¹⁸⁴Os (0.02%), ¹⁸⁶Os (1.59%), 187 Os (1.96%), 188 Os (13.24%), 189 Os (16.15%), ¹⁹⁰Os (26.26%), ¹⁹²Os (40.78%), one of which (¹⁸⁶Os) is a radioisotope with a half-life of 2.011×10^{15} years (α -decay), and for practical purposes is considered 'stable'. Of the stable isotopes, 187 Os and 189 Os possess a nuclear spin (I = $\frac{1}{2}$ and $\frac{3}{2}$, respectively), making them both magnetically receptive. 30 189 Os has a high quadrupole moment (Q = 0.91) and low gyromagnetic ratio (Table 1), making it relatively insensitive to detection (1.43×10^{-3}) at natural abundance relative to ¹³C), due to quadrupolar relaxation. ¹⁸⁹Os is therefore unsuitable for most NMR studies, with the exception of highly symmetrical molecules like 189OsO4, which yields a broad signal.

¹⁸⁷Os is a radioactive decay product of ¹⁸⁷Re (half-life of 4.56×10^{10} years) and has been studied extensively in the dating of terrestrial and meteoric rocks, and hydrocarbon deposits.³¹ It is an $I = \frac{1}{2}$ nucleus capable of yielding sharp NMR peaks over a chemical shift range of >5000 ppm. Bell et al. demonstrated that the use of polarisation transfer techniques to observe $J(^{187}\text{Os}-^{1}\text{H}/^{31}\text{P})$ couplings can greatly enhance the

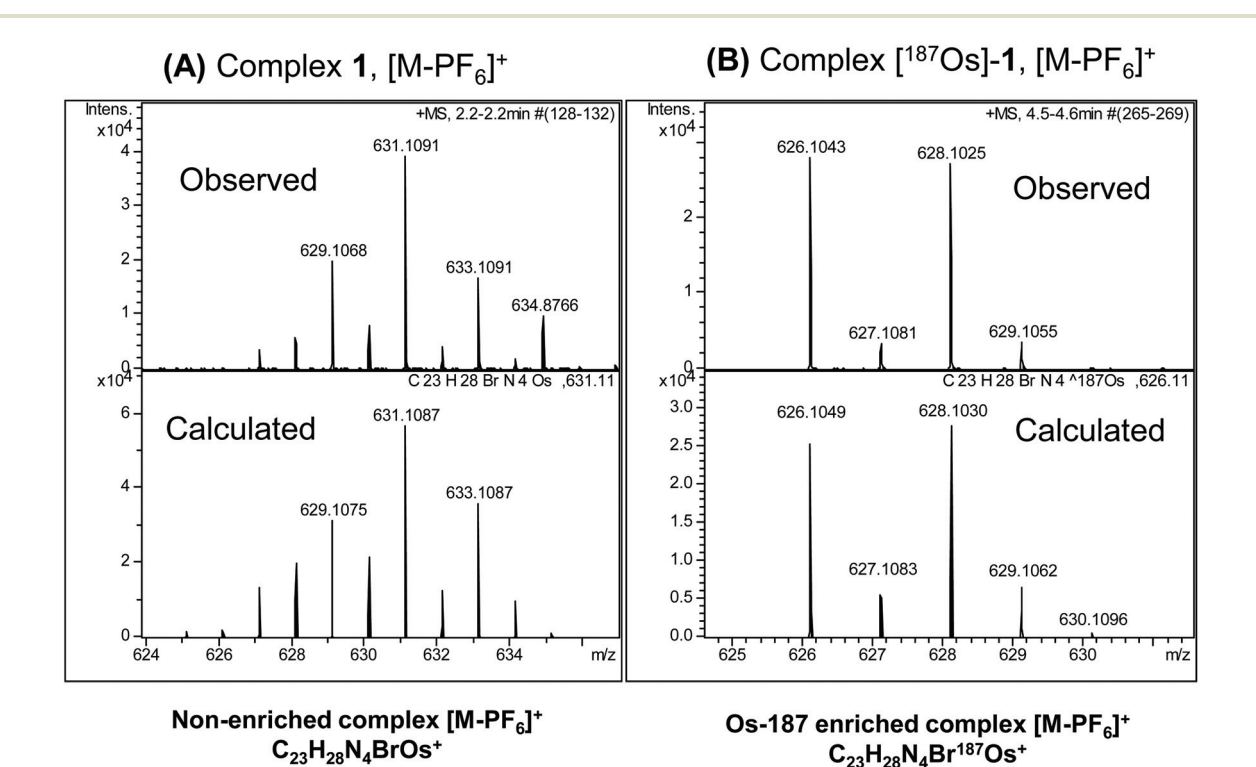


Fig. 2 Observed and calculated positive-ion high resolution mass spectra of (A) natural abundance complex 1 ([M - PF₆]⁺; [C₂₃H₂₈N₄BrOs]⁺), and (B) 187 Os-enriched $[^{187}$ Os]-1 ([M - PF₆]⁺; [C₂₃H₂₈N₄Br¹⁸⁷Os]⁺). The simplification of the spectrum on enrichment due to the presence of predominantly only one osmium isotope (187Os) together with 79Br (51%) and 81Br (49%) is apparent.

Dalton Transactions Paper

sensitivity of 187Os detection, with maximum gains of 1300 and 12 000 for ³¹P and ¹H-detected spectra. ³² This polarisation transfer approach had been applied also to u-hydrido and Cp complexes. 32-34 Bell et al. utilised one-bond 187Os-1H (hydride) couplings of ca. 70 Hz, and ¹⁸⁷Os-³¹P couplings to phosphines of ca. 270 Hz, to detect ¹⁸⁷Os NMR peaks for 37 [Os(arene) X₂(PR₃)] complexes. In a previous study on the biphenyl sandwich complex $[Os(n^6-bip)_2](OTf)_2$, we used ${}^1H/{}^{187}Os$ heteronuclear multiple bond correlation (HMBC) spectroscopy to observe the 187Os resonance for a 25 mM solution of the complex via the small ¹⁸⁷Os-¹H couplings to arene ring protons.35

Here we have synthesised the bromido analogue of the iodido complex FY26, $[Os(\eta^6-p-cym)(N,N-azpy-NMe_2)Br]PF_6$ (1), and determined its X-ray crystal structure. Also we have synthesised on a milligram scale, the ¹⁸⁷Os isotopically-enriched complex [187Os]-1, carried out multinuclear NMR and MS studies, and determined the antiproliferative activity of 1 towards human cancer cells. This appears to be the first report of NMR studies on a 187Os-enriched complex.

Results and discussion

Synthesis and characterisation

The synthesis of the ¹⁸⁷Os isotopically-enriched complex, $[^{187}\text{Os}(\eta^6-p\text{-cym})(N,N\text{-azpy-NMe}_2)\text{Br}]\text{PF}_6 \quad ([^{187}\text{Os}]\text{-1}), \quad \text{from} \quad ca.$ 50 mg metallic osmium-187 (98% enriched) was achieved in five steps based on previously reported methods (Scheme 1), with an overall yield of 41%. 36,37 The non-enriched complex 1 was synthesised from K₂[OsO₂(OH)₄], also via reported methods, and is analogous to the highly active complex $[Os(\eta^6 - \eta^6)]$ p-cym)(N,N-azpy-NMe₂)I]PF₆ (FY26),²¹ with bromide replacing iodide as the monodentate ligand.

The X-ray crystal structure of complex 1 shows that it adopts a similar pseudo-octahedral three-legged piano-stool geometry to its analogue, FY26, (Fig. 1, Table S1†).25 Osmium(II) is π -bonded to a p-cym ligand, and coordinated to a monodentate bromide and a bidentate azopyridine ligand, which constitute the three legs of the piano-stool. The complex crystallises as a racemate owing to the chiral Os centre, and contains a PF₆⁻ counter-anion.

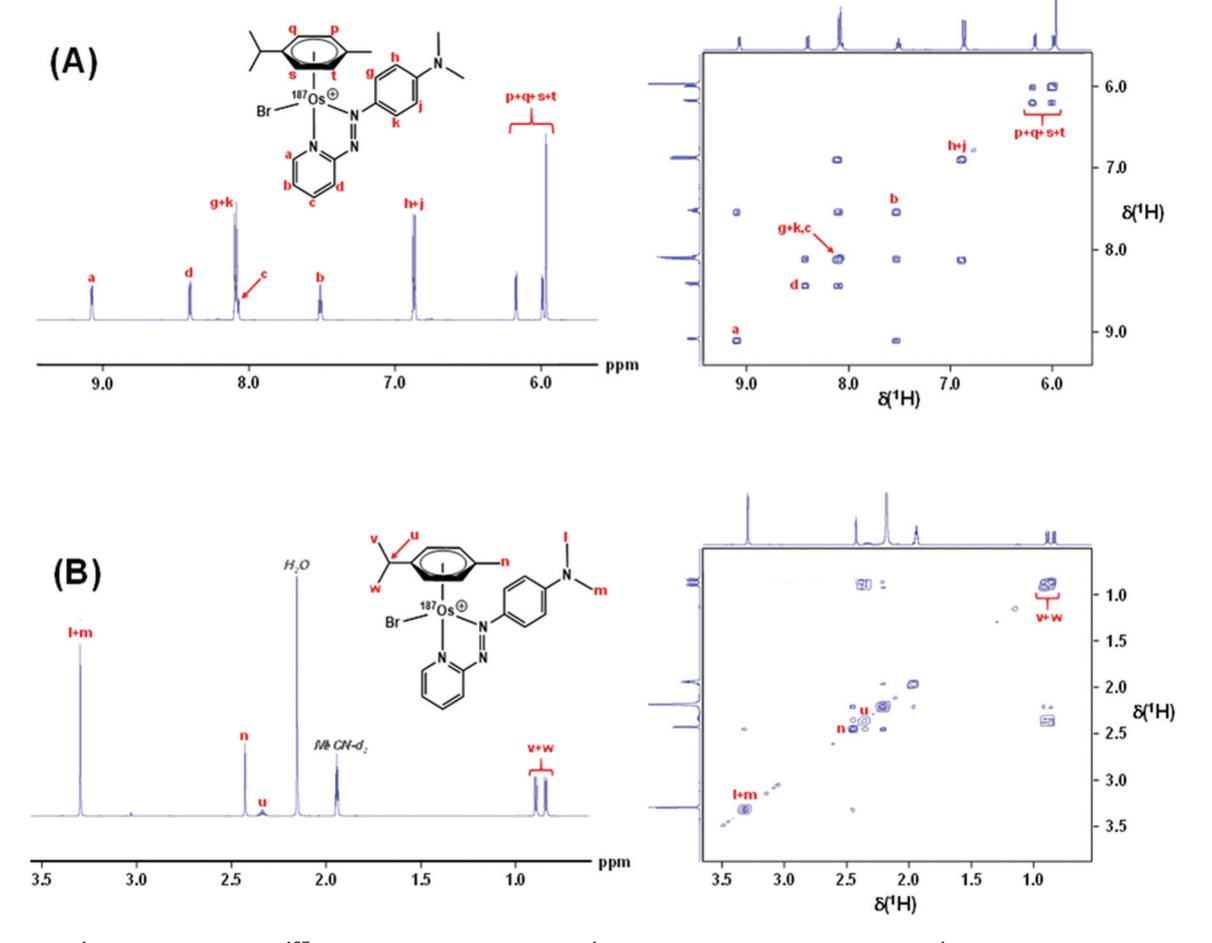


Fig. 3 700 MHz ¹H NMR spectrum of [¹⁸⁷Os]-1 (LHS), and 400 MHz 2D ¹H COSY NMR spectrum of 1 with all ¹H resonances assigned. (A) The aromatic region, and (B) the aliphatic region. Samples were prepared in MeCN- d_3 .

Anticancer activity

Paper

Similarly to FY26, complex 1 exhibits potent sub-micromolar antiproliferative activity against A2780 human ovarian cancer cells (IC $_{50}$ = 0.40 ± 0.01 μ M, 24 h drug exposure, 72 h recovery) and probably has a similar mechanism of action, inducing formation of reactive oxygen species (ROS) and perturbing the redox balance in cancer cells. The IC $_{50}$ follows an expected trend of activity for change in the monodentate ligand: I > Br > Cl, whereby the iodido complex is the most active and the chlorido complex is the least, due to weakening of the Os–X bond decreasing stability, and hence greater drug deactivation before reaching the target sites (Table S2†). This trend was

observed previously for a related bromido Os(II) arene azopyri-

dine complex and its halido analogues.³⁸ The racemic nature of the complex would be expected to have little effect on activity, since previous studies on the separated enantiomers of FY26 showed that the chiral centre does not significantly change the anticancer activity.³⁹

Mass spectrometry

The observed and calculated positive-ion high resolution mass spectra of natural abundance complex $\mathbf{1}$ ($[M - PF_6]^+$; $[C_{23}H_{28}N_4BrOs]^+$) and $[^{187}Os]^-\mathbf{1}$ ($[M - PF_6]^+$; $[C_{23}H_{28}N_4Br^{187}Os]^+$) are compared in Fig. 2A and B, respectively. The spectrum of enriched $[^{187}Os]^-\mathbf{1}$ is greatly simplified due to the presence of predominantly only one osmium isotope (^{187}Os) instead of 4

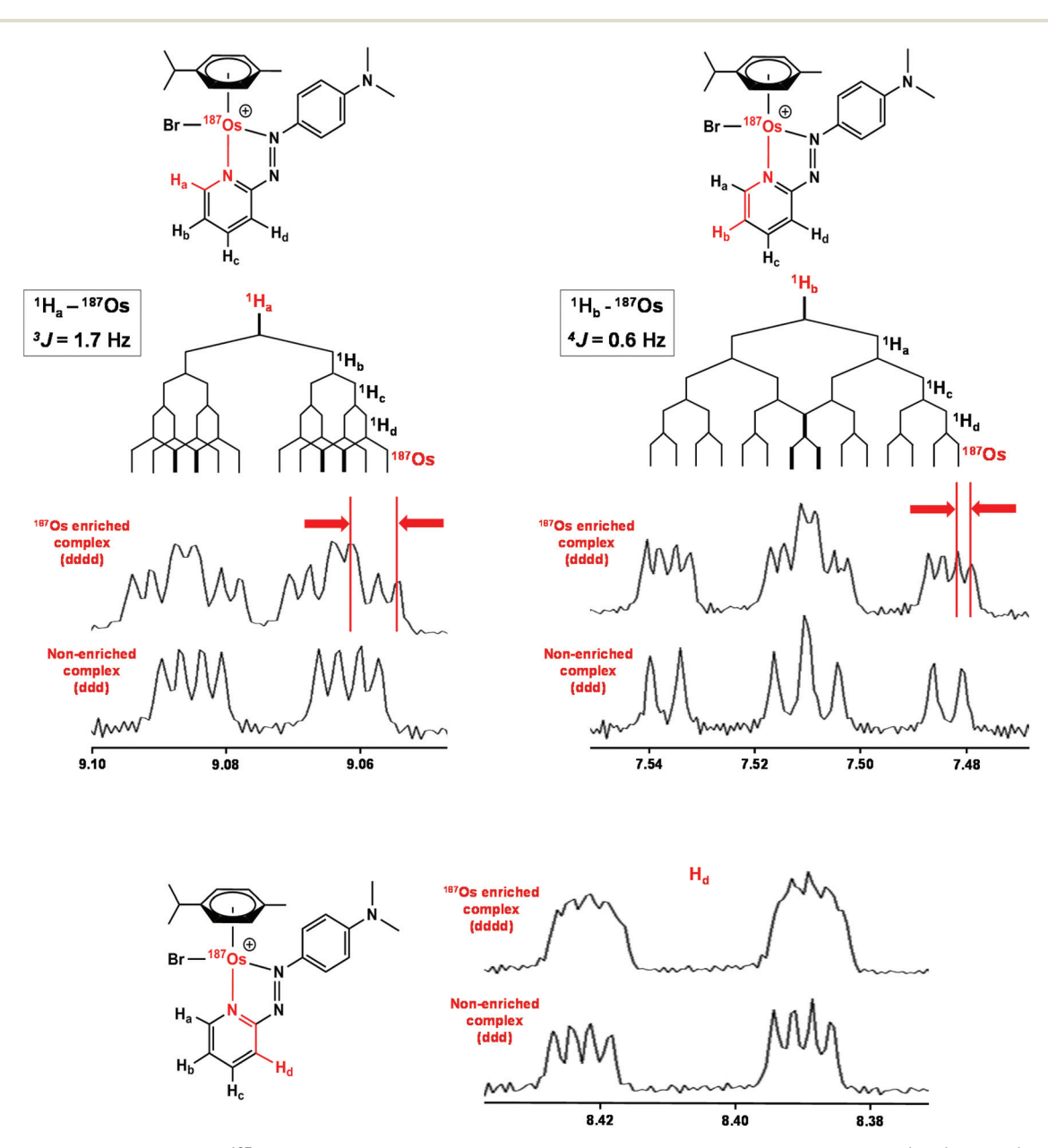


Fig. 4 1 H NMR (250 MHz) spectra of [187 Os]-1 compared to natural abundance 1, with expansions of the resonances for 1 H_a, 1 H_b, and 1 H_d illustrating their couplings to other protons and 187 Os. Samples were prepared in MeCN- d_3 .

Dalton Transactions Paper

additional isotopes (188Os 13.24%, 189Os 16.15%, 190Os 26.26%, and ¹⁹²Os 40.78%). The presence of ⁷⁹Br (natural abundance 51%) and ⁸¹Br (49%) isotopes is apparent.

¹H NMR

Complexes 1 and $[^{187}Os]$ -1 were prepared in MeCN- d_3 (~10 mg mL⁻¹) and ¹H COSY NMR spectra were recorded on 400 and 700 MHz instruments (Fig. 3), and the resonances assigned. To resolve coupling interactions between ¹⁸⁷Os and ¹H nuclei, 250 MHz ¹H NMR spectra of the samples were also recorded (Fig. 4). As expected, no ¹⁸⁷Os-¹H coupling interactions were observed for 1 due to the low natural abundance of ¹⁸⁷Os (1.96%). However, the ¹H spectrum of [¹⁸⁷Os]-1 shows the presence of 3- and 4-bond couplings between ¹⁸⁷Os and ${}^{1}\text{H}_{a}$ (${}^{3}\text{J} = 1.7 \text{ Hz}$), and ${}^{1}\text{H}_{b}$ (${}^{4}\text{J} = 0.6 \text{ Hz}$). There was also a small unresolved coupling to ¹H_d; the resolution was not sufficient to measure ⁴J. The resonance for proton ¹H_c is overlapped with other resonances, although the ⁵J value might be expected to be very small compared to the linewidth.

¹³C NMR

The samples used for ¹H NMR studies were also analysed by ¹³C NMR, utilising a J-MOD sequence (Fig. 5). To aid characterisation of the resonances, a ¹³C-¹H HMQC NMR spectrum was recorded (Fig. S1†), and all 23 13C resonances were observed and characterised in the spectrum. Furthermore, expansions of some resonances reveal distinct 187Os-13C couplings for

[187Os]-1 (Fig. 6). Short-range couplings are observed between ¹⁸⁷Os and ¹³C_p, ¹³C_q, ¹³C_s, and ¹³C_t (${}^{1}J = 7.2 - 8.0 \text{ Hz}$), which comprise the four CH carbons of the arene ring of the p-cym ligand, and between 187Os and the two tertiary carbons of the ring, $^{13}\text{C}_{\text{o}}$ and $^{13}\text{C}_{\text{r}}$ (^{1}J = 4.7 and 5.9 Hz, respectively). Furthermore, longer range couplings are observed between 187 Os and 13 C_e and 13 C_f (2 J = 2.4 and 5.0 Hz, respectively), and between 187 Os and 13 C_b (^{3}J = 1.8 Hz), which comprise 13 C resonances of the bidentate azpy ligand. Table 2 lists all the observed ¹⁸⁷Os-¹H and ¹⁸⁷Os-¹³C couplings.

¹H-¹⁸⁷Os HMBC

Utilising ¹H-¹⁸⁷Os HMBC, we were able to observe the ¹⁸⁷Os resonance of [187Os]-1 and determine its chemical shift relative to OsO₄. The resonance was observed at -4671.3 ppm through correlation with aromatic proton H_a (pyridyl ring), and aliphatic protons from the arene ligand, H_n (Fig. 7). Attempts to observe directly the ¹⁸⁷Os resonance of [¹⁸⁷Os]-1 were unsuccessful (Fig. S2†). The very low gyromagnetic ratio of ¹⁸⁷Os makes direct observation difficult, despite the complex being isotopically enriched. Fig. 8 shows a comparison of ¹⁸⁷Os chemical shifts for various organo-osmium complexes with arene and cyclopentadienyl ligands. The comparatively low chemical shift of the (high-field-shifted) 187Os resonance of [187Os]-1, similar to a bis-biphenyl arene Os(II) sandwich complex, suggests a highly shielded 187Os nucleus, perhaps surprising on account of the presence of the strong π -acceptor

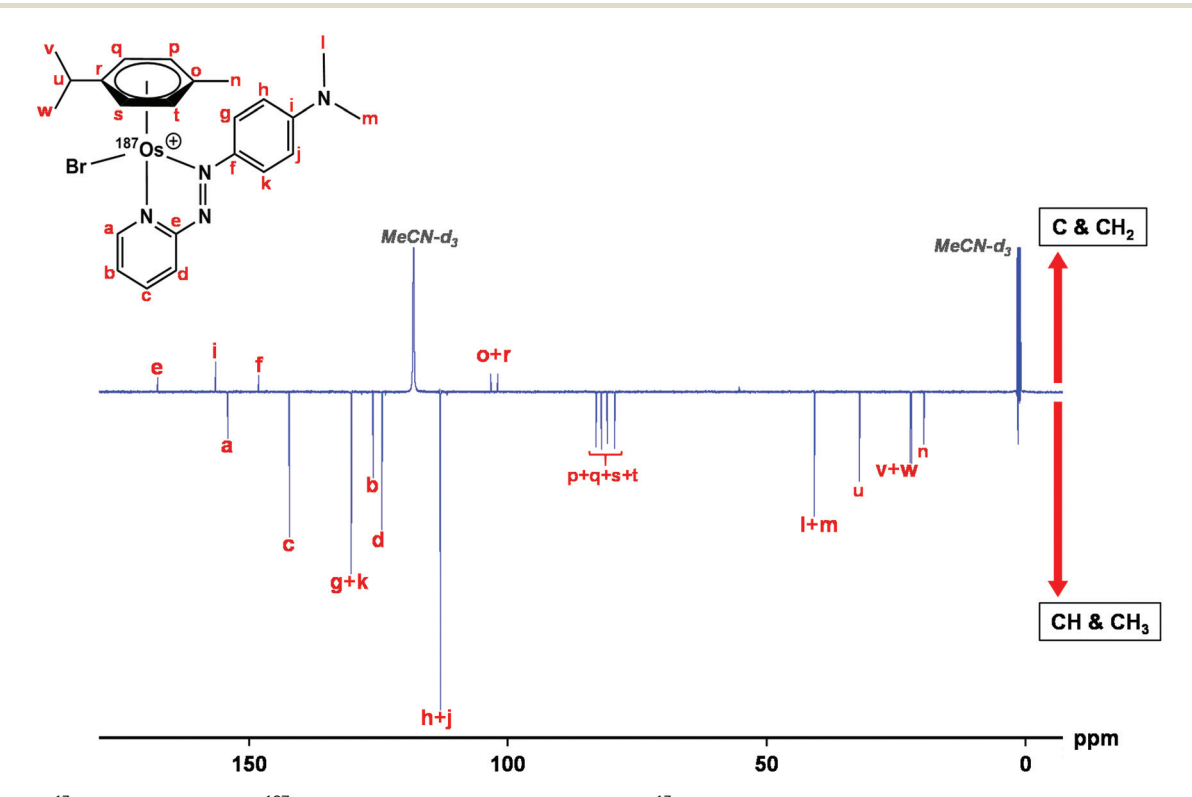


Fig. 5 176 Hz 13 C NMR spectrum of [187 Os]-1 using the J-MOD sequence, with 13 C assignments. The sample was prepared in MeCN- d_3 . C and CH₂ peaks are upright, CH and CH₃ peaks inverted.

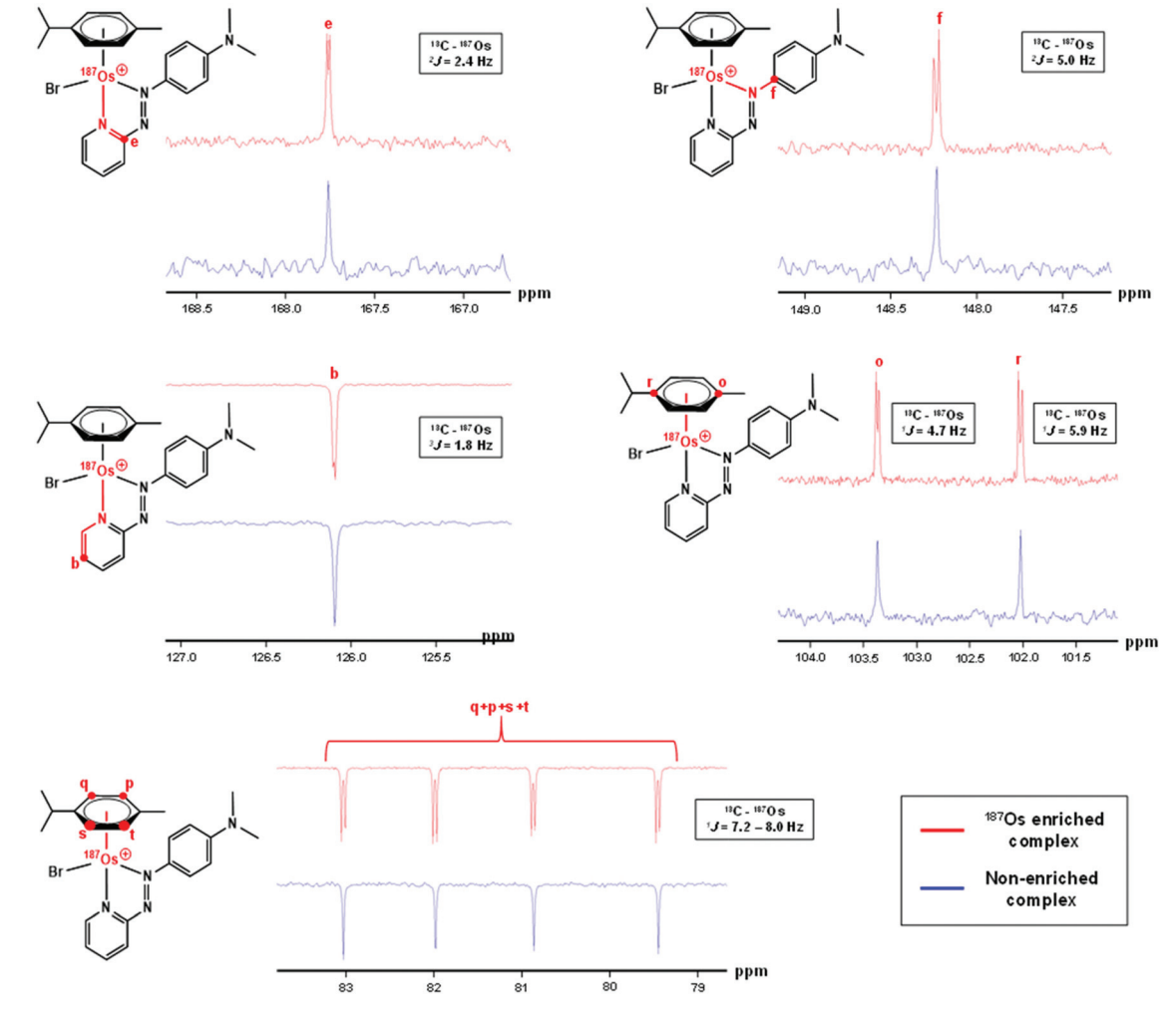


Fig. 6 176 MHz ¹³C NMR spectra of [¹⁸⁷Os]-1 compared to natural abundance 1 (150 MHz), with expansions of resonances for ¹³C_b, ¹³C_e, ¹³C_o, $^{13}C_p$, $^{13}C_q$, $^{13}C_r$, $^{13}C_s$, and $^{13}C_t$, which all exhibit couplings to ^{187}Os . Samples were prepared in MeCN- d_3 .

azopyridine ligand, although the comparator complexes mostly contain phosphines, or hydride ligands. Future work is required to elucidate the relationship between the electron densities in these complexes and the ¹⁸⁷Os chemical shifts, e.g. DFT calculations.

Heteronuclear NMR for metallodrugs

Most NMR spectroscopic studies of metallodrugs involve nuclei which are the most sensitive to detection. Only a few NMR nuclei offer the sensitivity for studies at pharmacological concentrations. These include ¹H, ¹⁹F, ³¹P, and ¹³C and ¹⁵N with enrichment and detection by polarisation transfer methods. Studies of NMR-active isotopes of metals present significant challenges.41-43

Sensitivity is a function of the size of the gyromagnetic ratio $(\gamma, proportional to the frequency of detection of resonances),$ the natural abundance, and the applied magnetic field (B_0) . NMR signal intensity is proportional to $B_0^{3/2} \gamma^{5/2}$. In general, as nuclei become heavier, they have smaller gyromagnetic ratios and they become less sensitive to detection. The detection sensitivity of low abundance nuclei such as ¹³C and ¹⁵N, which are often coupled to more sensitive ¹H nuclei, can be greatly enhanced by use of spin-polarisation-transfer pulse sequences such as heteronuclear single quantum coherence (HSQC), e.g. for ¹⁵N by up to a factor of 306 $(|\gamma^{1}H|/|\gamma^{15}N|)^{5/2}$.

All elements in the periodic table from atomic number 1 to 103 have at least one isotope which possesses nuclear spin.^{29,44} Radioactivity can be a problem for some elements, although shielding by glass is adequate for tritium (3H), which has a higher gyromagnetic ratio than ¹H and is 1.21× more sensitive to detection. A more common problem is that nuclei with spin quantum numbers $>\frac{1}{2}$ (quadrupolar nuclei) in environments that are not symmetrical, usually suffer line broadening via interaction with electric field gradients. For nuclei with high quadrupole moments (e.g. 197Au), this can lead to extreme broadening making resonances very difficult, and sometimes almost impossible to detect. Line broadening can also be severe for paramagnetic metal complexes, especially complexes where the unpaired spins have long electron spin relaxation times (those detectable by EPR at

Table 2 $\,^{187}\mathrm{Os}$ $J\text{-}\mathrm{couplings}$ to $^{1}\mathrm{H}$ and $^{13}\mathrm{C}$ determined by $^{1}\mathrm{H}$ and $^{13}\mathrm{C}$ NMR

Coupling	J^{a} (Hz)
$^{3}J(^{1}H_{a} - ^{187}Os)$	1.7
$^{4}J(^{1}H_{b} - ^{187}Os)$	0.6
$^{1}J(^{13}C_{o} - ^{187}Os)$	4.7
$^{1}J(^{13}C_{r} - ^{187}Os)$	5.9
${}^{1}J({}^{13}C_{q,p,s,t} - {}^{187}Os)$	7.2-8.0
$^{2}J(^{13}C_{e} - ^{187}Os)$	2.4
$^{2}J(^{13}C_{f} - ^{187}Os)$	5.0
$^{3}J(^{13}C_{b} - ^{187}Os)$	1.8

^a The signs of the coupling constants have not been determined.

ambient temperature), and when there are exchange processes which occur at intermediate rates on the NMR timescale. The resonances of heavier nuclei can be broadened by chemical shift anisotropy relaxation mechanisms (e.g. $^{195}\mathrm{Pt}$ in square-planar complexes), which also broadens $^{195}\mathrm{Pt}$ satellites in $^{1}\mathrm{H}$ NMR spectra of Pt(II) ligands. Such broadening is proportional to B_0^2 so can make such satellites very broad at high frequencies (e.g. at 600 MHz versus 300 MHz). 45

There is also current pharmacological interest in the group 8 metal iron. Ferrocene in particular shows promise as a fragment for conjugation in drug design. 46,47 Ferroquine is on clinical trial as an antimalarial drug, 48 and ferrocifens (tamoxifen derivatives) have promising anticancer activity especially towards breast cancer cells possessing the estrogen receptor (ER+). 49 57 Fe is an $I = \frac{1}{2}$ nucleus, but the abundance is low (2.1%), as is the gyromagnetic ratio, Table 1. With polarisation transfer from 1H, utilising the small two-bond Cp (C-H) ¹H-⁵⁷Fe coupling of ca. 0.5 Hz, ⁵⁷Fe resonances can readily be detected for concentrated solutions of ferrocene (ca. 0.4 M). 50 57 Fe chemical shifts have been used to study the donor properties of amino groups on coordinated Cp rings.⁵¹ ⁵⁷Fe isotopic enrichment (to ca. 90%) allows detection at millimolar concentrations, e.g. for haem proteins.⁵² Enrichment combined with polarisation-transfer methods should allow detection at pharmacological concentrations of relevance to metallodrug activity. However, oxidation to paramagnetic 3d⁵ Fe(III) is likely to lead to severe broadening and loss of ⁵⁷Fe resonances.

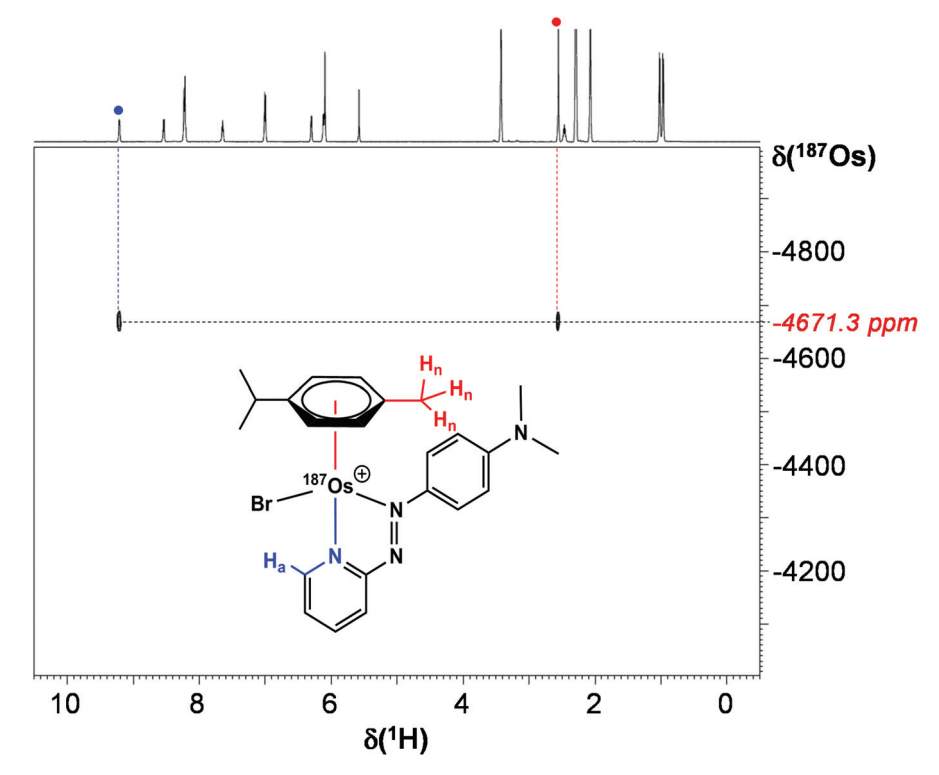


Fig. 7 2D $^{1}\text{H}-^{187}\text{Os HMBC NMR spectrum of }[^{187}\text{Os}]-1$ in MeCN- d_3 .

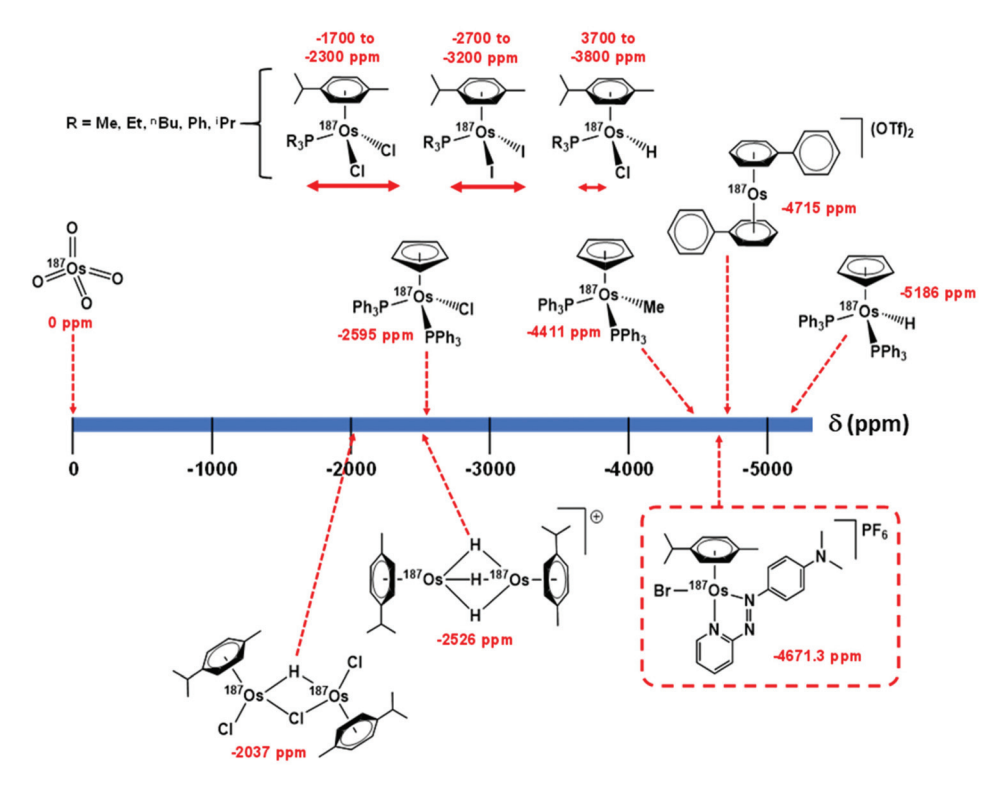


Fig. 8 Comparison of ¹⁸⁷Os chemical shifts for [¹⁸⁷Os]-1 in comparison with values for arene and cyclopentadienyl Os(II) complexes in the literature. 33–35,40 Shifts are either referenced directly to OsO₄ or indirectly from the proton frequency of TMS.

Conclusions

NMR is a versatile technique for the study of metallodrugs in both the solid state and solution. Here we have focussed on solution studies, which can not only provide structural information, but also insights into both the thermodynamics and kinetics of ligand exchange reactions. Such information is vital for identifying pharmacologically active species. The common spin $\frac{1}{2}$ nuclei 1H, 19F and 31P are sensitive enough for NMR studies at physiologically relevant concentrations (often sub-millimolar), and so too are 13C and 15N in isotopically-enriched compounds, especially when polarisation transfer methods such as HSQC are used. In contrast, $I > \frac{1}{2}$ (quadrupolar) nuclei usually give rise to broad peaks which limits their usefulness at low concentrations.

Platinum anticancer drugs are now the most widely used drugs in cancer chemotherapy, and NMR studies of the 33.4% abundant $I = \frac{1}{2}$ isotope ¹⁹⁵Pt have proved useful for studies of the activation of cisplatin and related drugs by hydrolysis and subsequent attack of DNA target sites, as well as the reduction of Pt(IV) prodrugs to Pt(II). 4,41,43,53 Currently, there is much interest in the discovery of active anticancer complexes of other transition metals, and we have highlighted here the potential for group 8 of the periodic table, iron, ruthenium, and osmium. Complexes of ruthenium have already entered clinical trials,54 and one is in clinical trials as a photosensitizer for cancer treatment. 10 However, ruthenium has only quadrupolar nuclei and direct studies of these drugs by Ru NMR are difficult. The heavier congener, osmium, on the other

hand has a useful $I = \frac{1}{2}$ isotope ¹⁸⁷Os, although with a low natural abundance and low gyromagnetic ratio (Table 1).

We have shown here that isotopic enrichment of a potent anticancer complex \lceil^{187} Os $(\eta^6$ -p-cym)(N,N-azpy-NMe₂)Br \rceil PF₆ to >98% ¹⁸⁷Os allows facile detection of its ¹⁸⁷Os resonance NMR using 2D ¹H-¹⁸⁷Os HMBC, and accompanying ¹H and ¹³C NMR studies allow detection for the first time of ${}^{1}J$, ${}^{2}J$, ${}^{3}J$ and ⁴J coupling constants for both the arene ring and the chelated azopyridine ligand, ranging from 0.6-8 Hz. However, despite isotopic enrichment, direct observation of the ¹⁸⁷Os resonance (without the use of spin-polarisation-transfer techniques) was not achievable due to its very low gyromagnetic ratio. The synthesis of the enriched complex was achieved in good yield over 5 steps from metallic ¹⁸⁷Os, the first step of which involved conversion to ¹⁸⁷OsO₄, a highly toxic volatile compound generated in a KOH/KNO3 melt at >350 °C. The mechanism of anticancer activity of this class of organo-osmium arene anticancer complexes appears to be different from that of platinum anticancer drugs, and further studies using such 187Os-enriched complexes are likely to provide new insight into their reactions in biological media and the nature of their target sites.

Experimental

Materials

Chemicals. ¹⁸⁷Os powder was the kind gift of Dr Dimitrios Bessas (ESRF, Grenoble). K₂[OsO₂(OH)₄] and N,N-dimethyl-4Dalton Transactions Paper

(2-pyridylazo)aniline were purchased from Alfa Aesar, and α -terpinene and ammonium hexafluorophosphate were purchased from Sigma-Aldrich. All other general reagents (KOH, KNO₃, and HBr), and organic solvents were purchased from commercial suppliers and used as received. Deionised water for synthesis was produced using a Millipore Elix 5 water purification system.

Cell culture. DMEM cell culture media, penicillin/streptomycin mixture, foetal bovine serum, L-glutamine, and trypsin were all purchased from PAA Laboratories GmbH. DMEM was supplemented with foetal bovine serum (50 mL), penicillin/streptomycin mixture (5 mL), and L-glutamine (5 mL). The A2780 cell line was purchased from the European Collection of Cell Cultures.

Synthesis

 $[^{187}Os(\eta^6-p\text{-cym})Br_2]_2$. Powdered osmium-187 (50.3 mg, 0.267 mmol), KOH (0.5 g) and KNO₃ (0.3 g) were mixed in an alumina crucible and heated to 350-400 °C, yielding a brown melt. After cooling to ambient temperature the solids were dissolved in H₂O (10 mL). EtOH (20 mL) was added and a pinkpurple precipitate formed. The solvents were removed by decantation and the precipitate washed with EtOH: H2O (3:1, v/v, 3 × 15 mL). The clean precipitate was mixed with EtOH (10 mL), HBr (48%, v/v, 5 mL) and heated under reflux for 18 h. α-Terpinene (501 mg, 3.678 mmol) was added and the mixture was refluxed for a further 18 h. The product was extracted with CH2Cl2 (25 mL) and washed with H2O (3 × 20 mL). The solution was concentrated to ~3 mL under reduced pressure and a brown precipitate formed, which was placed in a freezer overnight (253 K). The precipitate was collected via vacuum filtration and washed with EtOH (5 mL) and Et₂O (5 mL). Yield (53.1 mg, 41%). No analysis was conducted at this stage to avoid loss of valuable ¹⁸⁷Os. *Note*: Extreme care must be taken with the handling of the OsO4 intermediate

Natural abundance $[Os(\eta^6-p\text{-cym})Br_2]_2$ was synthesised from $K_2[OsO_2(OH)_4]$ using a previously reported method.³⁷

 $[^{187}Os(\eta^6-p\text{-cym})(N,N\text{-azpy-NMe}_2)Br]PF_6.$ $[^{187}Os(\eta^6-p\text{-cym})]$ Br_2 ₂ (12.6 mg, 13.10 µmol) was dissolved in EtOH (10 mL), and a solution of N,N-dimethyl-4-(2-pyridylazo)aniline (6.2 mg, 27.322 µmol) in EtOH (5 mL) was added drop-wise to the stirred mixture. The mixture was stirred at 313 K for 2 h, then NH₄PF₆ (21.2 mg, 0.130 mmol) was added. The mixture was concentrated to ~2 mL under reduced pressure and placed in a freezer overnight (253 K). A dark blue precipitate formed, which was collected via vacuum filtration and washed with icecold EtOH (1 mL) and Et₂O (5 mL). The product was dried in a vacuum desiccator overnight. Yield: (18.6 mg, 92%). ¹H NMR 250 MHz (CD₃CN): δ 9.07 (dddd, 1H, J = 5.8, 1.6, 1.7, 1.0 Hz), 8.41 (m, 1H), 8.05–8.13 (m, 3H), 7.51 (dddd, 1H, J = 7.5, 5.9, 1.4, 0.6 Hz), 6.84-6.90 (m, 2H), 6.16-6.18 (m, 1H), 5.95-6.00 (m, 3H), 3.30 (s, 6H), 2.43 (s, 3H), 2.34 (sept., 1H, J = 6.9 Hz), 0.90 (d, 3H, J = 6.9 Hz), 0.85 (d, 3H, J = 6.9 Hz). ¹³C NMR 176 MHz (CD₃CN): δ 167.75 (C), 156.56 (C), 154.21 (CH), 148.23 (C), 142.31 (CH), 130.33 (CH), 126.09 (CH), 124.41 (CH),

113.10 (*CH*), 103.36 (*C*), 102.02 (*C*), 83.03 (*CH*), 81.98 (*CH*), 80.87 (*CH*), 79.45 (*CH*), 40.83 (*CH*₃), 32.08 (*CH*), 22.27 (*CH*₃), 22.06 (*CH*₃), 19.64 (*CH*₃). ESI-MS calculated for $C_{23}H_{28}BrN_4^{187}Os^+: m/z$ 626.1049. Found: 626.1043.

Natural abundance $[Os(\eta^6-p\text{-cym})(N,N\text{-azpy-NMe}_2)Br]PF_6$

Synthesised using the same procedure as above with; $[Os(\eta^6-p$ cym) Br_2 ₂ (58.6 mg, 60.548 µmol), N,N-dimethyl-4-(2-pyridylazo)aniline (30.1 mg, 133.120 μmol), and NH₄PF₆ (98.6 mg, 0.605 mmol). Yield: (79.9 mg, 85%). ¹H NMR 250 MHz (CD₃CN): δ 9.07 (ddd, 1H, J = 5.8, 1.4, 0.6 Hz), 8.41 (ddd, 1H, J= 8.2, 1.3, 0.6 Hz), 8.05-8.13 (m, 3H), 7.51 (ddd, 1H, J = 7.5,5.9, 1.4 Hz), 6.84-6.90 (m, 2H), 6.16-6.18 (m, 1H), 5.96-6.00 (m, 3H), 3.30 (s, 6H), 2.43 (s, 3H), 2.34 (sept., 1H, <math>J = 6.9 Hz),0.90 (d, 3H, J = 6.9 Hz), 0.85 (d, 3H, J = 6.9 Hz). ¹³C NMR 150 MHz (CD₃CN): δ 167.75 (C), 156.56 (C), 154.20 (CH), 148.23 (C), 142.31 (CH), 130.33 (CH), 126.09 (CH), 124.41 (CH), 113.10 (CH), 103.36 (C), 102.01 (C), 83.02 (CH), 81.98 (CH), 80.86 (CH), 79.44 (CH), 40.83 (CH₃), 32.08 (CH), 22.27 (CH₃), $(CH_3),$ 19.63 (CH_3). ESI-MS calculated $C_{23}H_{28}BrN_4Os^+$: m/z 631.1087. Found: 631.1091. CHN analysis: Found: C, 35.37%; H, 3.44%; N, 7.37%. Calculated for C₂₃H₂₈BrF₆N₄OsP: C, 35.62%; H, 3.64%; N, 7.22%.

X-ray crystal structure

A single crystal of complex 1 was grown by slow evaporation of a methanolic solution (~3 mg mL⁻¹), and its molecular structure was determined by X-ray crystallography (Fig. 1). Diffraction data were collected on an Oxford Diffraction Gemini four-circle system with a Ruby CCD area detector. The structure was refined by full-matrix least squares against F2 using SHELXL 97 and solved by direct methods using SHELXS (TREF) with additional light atoms found by Fourier methods.55 Hydrogen atoms were added at calculated positions and refined using a riding model. Anisotropic displacement parameters were used for all non-H atoms; H-atoms were given an isotropic displacement parameter equal to 1.2 (or 1.5 for methyl and NH H-atoms) times the equivalent isotropic displacement parameter of the atom to which they are attached. The data were processed by the modelling program Mercury 1.4.1. X-ray crystallographic data for complex 1 have been deposited in the Cambridge Crystallographic Data Centre under the accession number CCDC 2067332.†

Mass spectrometry

Electrospray mass spectra were obtained using a Bruker MaXis UHR-ESI-TOF instrument. Samples of 1 and [187 Os]-1 were prepared in methanol and analysed in positive ion mode ($500-1000 \ m/z$).

NMR spectroscopy

 1 H and 13 C NMR spectra were acquired in 5 mm NMR tubes at 298 K on Bruker AV-250, AV-400, AV-600 or AV-700 spectrometers in MeCN- d_3 . Data processing was carried out using TOPSPIN version 2.1 (Bruker UK Ltd). 1 H NMR chemical shifts were internally referenced to TMS via the residual solvent

peak: acetonitrile (δ = 1.94 ppm).⁵⁶ Likewise for ¹³C NMR chemical shifts: acetonitrile (δ = 1.32 ppm). 1D ¹H NMR spectra were recorded using standard pulse sequences and 1D ¹³C NMR spectra were recorded using a J-MOD pulse sequence. Typically, ¹H data were acquired with 16 transients into 32k data points over a spectral width of 14 ppm, and ¹³C data with 8192 transients into 64k data points over a spectral width of 220 ppm.

¹H-¹⁸⁷Os HMBC NMR spectroscopy was carried out with MeCN- d_3 as solvent at 298 K on an Advance III 600 (1 H = 600.13 MHz, ¹⁸⁷Os = 13.69 MHz) spectrometer equipped with a 5 mm triple resonance broadband inverse (TBI-Lr) ¹H/³¹P/BB probe with z-field gradients. The 90° pulse length for ¹⁸⁷Os was 11 µs. The 187Os resonance frequency was roughly estimated from a series of ¹H-¹⁸⁷Os HMBC experiments carried out with incremented values of the carrier frequency. In order to check for the absence of folding in the F1 dimension, two gradient-enhanced HMBC spectra were recorded with different settings of the ¹⁸⁷Os spectral width and offset (SW = 1000 ppm O1P = -3800 and -4500 respectively). The second, shown in Fig. 7, was recorded with the following experimental conditions: 128 transients collected for each FID, 32 increments, 1/2J delay set to 0.1 s, recycling delay 2.25 s; three sine-shaped gradients pulses of 1 ms duration in the intensity ratio of 60:20:41.83 for coherence (echo type) selection; sine bell multiplication in both dimensions and zero filling to 1024 data points in the F1 dimension was applied before Fourier transform followed by magnitude calculation. The reference frequency for the 187Os chemical shift was calculated from the proton frequency of internal TMS, using a conversion factor Ξ = 2.282331.

¹⁸⁷Os NMR spectroscopy was carried out using MeCN-d₃ as solventat 298 K on an Avance III 600 (¹H = 600.13 MHz, ¹⁸⁷Os = 13.69 MHz) spectrometer equipped with a 5 mm triple resonance broadband inverse (TBI-Lr) ¹H/³¹P/BB probe with z-field gradients. The 90° pulse length for osmium was 11 μs. A series of experiments was carried out with incremented values of the carrier frequency in order to scan the full 10 000 ppm scale (SW = 1000 ppm O1P = from 4500 to -4500). A standard 1D sequence with power gated decoupling was used with 256 scans, recycling delay 4 s.

Cytotoxicity assay

A stock solution of 1 was prepared in cell culture medium (5% DMSO). Approximately 5000 A2780 human ovarian cancer cells were seeded per well in 96-well plates. The cells were pre-incubated in drug-free media at 37 °C for 48 h before adding different concentrations of 1. Cells were exposed to 1 for 24 h at 37 °C and then allowed to recover for 72 h in a drug-free medium at 37 °C. Then the supernatants were removed by suction and the cells washed with PBS. The cells were The SRB assay was used to determine cell viability. Absorbance measurements of the solubilised dye (on a BioRad iMark microplate reader using a 470 nm filter) allowed the determination of viable treated cells compared to untreated controls. IC₅₀ values (the concentration at which 50% cell death occurs)

were determined as triplicates of duplicates for each complex. ICP-OES (PerkinElmer Optima 5300 DV instrument) was used to determine [Os] of the stock solution of 1, and the IC₅₀ value was corrected for ICP factor.

Conflicts of interest

There are no conflicts of interest.

Acknowledgements

We thank the EPSRC (grant no. EP/F034210/1 and EP/P030572/ 1), ERC (grant no. 247450), and Anglo American Platinum for their support for this work, and Dr Dimitrios Bessas (ESRF) for his kind gift of osmium-187. We are grateful to Dr Lijiang Song for assistance with mass spectrometry.

References

- 1 K. D. Mjos and C. Orvig, Chem. Rev., 2014, 114, 4540-4563.
- 2 C. Imberti and P. J. Sadler, in Adv. Inorg. Chem, ed. P. J. Sadler and R. van Eldik, Academic Press, 2020, vol. 75, pp. 3-56.
- 3 R. J. Needham and P. J. Sadler, in The Periodic Table II: Catalytic, Materials, Biological and Medical Applications, ed. D. M. P. Mingos, Springer International Publishing, Cham, 2019, pp. 175-201.
- 4 E. J. Anthony, E. M. Bolitho, H. E. Bridgewater, O. W. L. Carter, J. M. Donnelly, C. Imberti, E. C. Lant, F. Lermyte, R. J. Needham, M. Palau, P. J. Sadler, H. Shi, F.-X. Wang, W.-Y. Zhang and Z. Zhang, Chem. Sci., 2020, 11, 12888-12917.
- 5 E. Alessio and L. Messori, in Metallo-Drugs: Development and Action of Anticancer Agents, ed. S. Astrid, S. Helmut, F. Eva and K. O. S. Roland, De Gruyter, 2018, pp. 141-170.
- 6 K. J. Ooms and R. E. Wasylishen, J. Am. Chem. Soc., 2004, 126, 10972-10980.
- 7 C. Brevard and P. Granger, *Inorg. Chem.*, 1983, 22, 532–535.
- 8 X. Xiao, M.-I. Takeko and M. Shigeo, Chem. Lett., 1997, 26, 241-242.
- 9 G. Orellana, A. Kirsch-De Mesmaeker and N. J. Turro, Inorg. Chem., 1990, 29, 882-885.
- 10 S. Monro, K. L. Colón, H. Yin, J. Roque 3rd, P. Konda, S. Gujar, R. P. Thummel, L. Lilge, C. G. Cameron and S. A. McFarland, Chem. Rev., 2019, 119, 797-828.
- 11 https://clinicaltrials.gov/ct2/show/NCT03945162.
- 12 http://kodu.ut.ee/~laurit/AK2/NMR_tables_Bruker2012.pdf.
- 13 S. M. Meier-Menches, C. Gerner, W. Berger, C. G. Hartinger and B. K. Keppler, Chem. Soc. Rev., 2018, 47, 909-928.
- 14 M. Hanif, M. V. Babak and C. G. Hartinger, Drug Discovery Today, 2014, 19, 1640-1648.
- 15 T. C. Johnstone, K. Suntharalingam and S. J. Lippard, Philos. Trans. R. Soc., A, 2015, 373, 20140185.

16 W. X. Ni, W. L. Man, M. T. Cheung, R. W. Sun, Y. L. Shu,

Y. W. Lam, C. M. Che and T. C. Lau, Chem. Commun., 2011, 47, 2140-2142.

Dalton Transactions

- 17 K. Suntharalingam, T. C. Johnstone, P. M. Bruno, W. Lin, M. T. Hemann and S. J. Lippard, J. Am. Chem. Soc., 2013, 135, 14060-14063.
- 18 A. Dorcier, C. G. Hartinger, R. Scopelliti, R. H. Fish, B. K. Keppler and P. J. Dyson, J. Inorg. Biochem., 2008, 102, 1066-1076.
- 19 E. Păunescu, P. Nowak-Sliwinska, C. M. Clavel, R. Scopelliti, A. W. Griffioen and P. J. Dyson, ChemMedChem, 2015, 10, 1539-1547.
- 20 H. Kostrhunova, J. Florian, O. Novakova, A. F. A. Peacock, P. J. Sadler and V. Brabec, J. Med. Chem., 2008, 51, 3635-3643
- 21 Y. Fu, A. Habtemariam, A. M. Pizarro, S. H. van Rijt, D. J. Healey, P. A. Cooper, S. D. Shnyder, G. J. Clarkson and P. J. Sadler, J. Med. Chem., 2010, 53, 8192-8196.
- 22 J. M. Hearn, I. Romero-Canelón, A. F. Munro, Y. Fu, A. M. Pizarro, M. J. Garnett, U. McDermott, N. O. Carragher and P. J. Sadler, Proc. Natl. Acad. Sci. U. S. A., 2015, 112, E3800-E3805.
- 23 S. D. Shnyder, Y. Fu, A. Habtemariam, S. H. van Rijt, P. A. Cooper, P. M. Loadman and P. J. Sadler, MedChemComm, 2011, 2, 666-668.
- 24 I. Romero-Canelón, M. Mos and P. J. Sadler, J. Med. Chem., 2015, 58, 7874-7880.
- 25 R. J. Needham, C. Sanchez-Cano, X. Zhang, I. Romero-Canelón, A. Habtemariam, M. S. Cooper, L. Meszaros, G. J. Clarkson, P. J. Blower and P. J. Sadler, Angew. Chem., Int. Ed., 2017, 56, 1017-1020.
- 26 J. P. C. Coverdale, C. Sanchez-Cano, G. J. Clarkson, R. Soni, M. Wills and P. J. Sadler, Chem. - Eur. J., 2015, 21, 8043-8046.
- 27 J. P. C. Coverdale, I. Romero-Canelón, C. Sanchez-Cano, G. J. Clarkson, A. Habtemariam, M. Wills and P. J. Sadler, Nat. Chem., 2018, 10, 347-354.
- 28 G. Girolami, Nat. Chem., 2012, 4, 954-954.
- 29 https://www.webelements.com/isotopes.html.
- 30 http://mriquestions.com/predict-nuclear-spin-i.html.
- 31 D. Selby and R. A. Creaser, Science, 2005, 308, 1293-1295.
- 32 A. G. Bell, W. Koźmiński, A. Linden and W. von Philipsborn, Organometallics, 1996, 15, 3124-3135.
- 33 J. A. Cabeza, B. E. Mann, P. M. Maitlis and C. Brevard, J. Chem. Soc., Dalton Trans., 1988, 629-634.
- 34 A. Gisler, M. Schaade, E. J. M. Meier, A. Linden and W. von Philipsborn, J. Organomet. Chem., 1997, 545-546, 315-326.

- 35 J. C. Gray, A. Pagelot, A. Collins, F. P. A. Fabbiani, S. Parsons and P. J. Sadler, Eur. J. Inorg. Chem., 2009, 2009, 2673-2677.
- 36 H. L. Grube, in Handbook of Preparative Inorganic Chemistry, ed. G. Brauer, Academic Press Inc., 1965, vol. 2, p. 1604.
- 37 H. S. Clayton, B. C. E. Makhubela, H. Su, G. S. Smith and J. R. Moss, Polyhedron, 2009, 28, 1511-1517.
- 38 R. J. Needham, H. E. Bridgewater, I. Romero-Canelón, A. Habtemariam, G. J. Clarkson and P. J. Sadler, J. Inorg. Biochem., 2020, 210, 111154.
- 39 S. A. Kumar, R. J. Needham, K. Abraham, H. E. Bridgewater, L. A. Garbutt, H. Xandri-Monje, R. Dallmann, S. Perrier, P. J. Sadler and F. Lévi, Metallomics, 2020, 13, mfaa003.
- 40 R. Benn, H. Brenneke, E. Joussen, H. Lehmkuhl and F. López Ortiz, Organometallics, 1990, 9, 756-761.
- 41 S. J. Berners-Price and P. J. Sadler, Coord. Chem. Rev., 1996, 151, 1-40.
- 42 L. Ronconi and P. J. Sadler, Coord. Chem. Rev., 2008, 252, 2239-2277.
- 43 T. Zou and P. J. Sadler, Drug Discovery Today: Technol., 2015, 16, 7-15.
- 44 http://mriquestions.com/predict-nuclear-spin-i.html.
- 45 I. M. Ismail, S. J. S. Kerrison and P. J. Sadler, Polyhedron, 1982, 1, 57-59.
- 46 G. Gasser, I. Ott and N. Metzler-Nolte, J. Med. Chem., 2011, **54**, 3-25.
- 47 P. Chellan and P. J. Sadler, Chem. Eur. J., 2020, 26, 8676-8688
- 48 D. Daniel and B. Christophe, Curr. Top. Med. Chem., 2014, 14, 1684-1692.
- 49 G. Jaouen, A. Vessières and S. Top, Chem. Soc. Rev., 2015, 44, 8802-8817.
- 50 B. Wrackmeyer, O. L. Tok and M. Herberhold, Organometallics, 2001, 20, 5774-5776.
- 51 B. Wrackmeyer, E. V. Klimkina, H. E. Maisel, O. L. Tok and M. Herberhold, Magn. Reson. Chem., 2008, 46, S30-S35.
- 52 L. Baltzer, E. D. Becker, R. G. Tschudin and O. A. Gansow, J. Chem. Soc., Chem. Commun., 1985, 1040-1041.
- 53 S. J. Berners-Price, L. Ronconi and P. J. Sadler, Prog. Nucl. Magn. Reson. Spectrosc., 2006, 49, 65-98.
- 54 A. Bergamo, C. Gaiddon, J. H. Schellens, J. H. Beijnen and G. Sava, J. Inorg. Biochem., 2012, 106, 90-99.
- 55 G. Sheldrick, Acta Crystallogr., Sect. A: Found. Crystallogr., 1990, 46, 467-473.
- 56 H. E. Gottlieb, V. Kotlyar and A. Nudelman, J. Org. Chem., 1997, 62, 7512-7515.